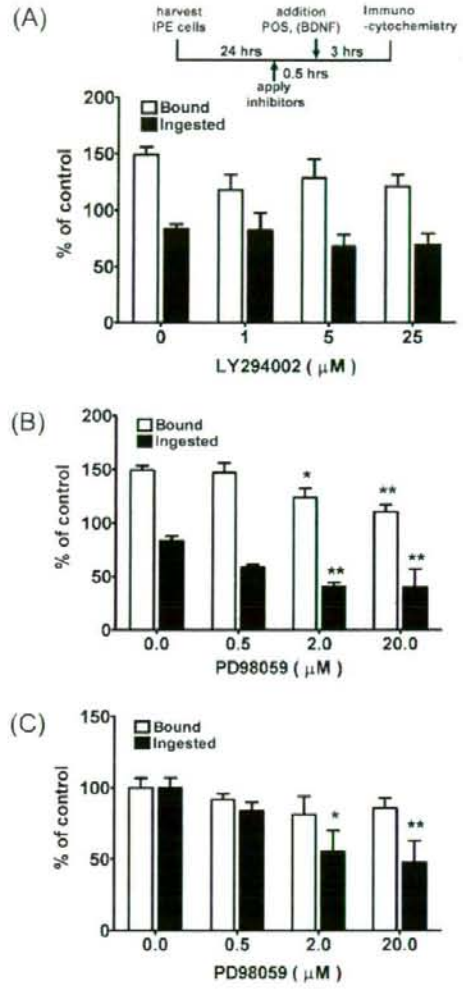

Fig. 2. Effect of protein kinase inhibitors on phagocytic activities in IPE cells cultured with or without BDNF. Each inhibitor was added to the medium 30 minutes before the challenge of POS and BDNF, and was contained for experimental periods. LY294002 did not affect both phagocytic activities of the binding and ingestion (A). In BDNF-treated IPE cells PD98059 inhibited both phagocytic activities of the binding and the ingestion (B). Only the binding phase of the phagocytosis in cultured IPE cells with growth medium without BDNF was inhibited by PD98059 (C). Statistical analysis was performed by the Bonferroni/Dunn multiple range test (*,**$p<0.05$, 0.01).

Discussion

In the present study, we found that BDNF specifically affected POS binding to IPE cells resulting in increased phagocytic activities in IPE cells. It is reported that the tyrosine kinase receptor, trkB, plays an important role in the signal transduction pathway of BDNF (Soppet *et al.*, 1991) which activates PI3K (Fryer *et al.*, 2000; Nakazawa *et al.*, 2002) and MAPK pathway (Barnabe-Heider and Miller, 2003; Hans *et al.*, 2004; Kelly-Spratt *et al.*, 1999). Our data suggest that increased POS binding activity of IPE cells caused by BDNF was mediated through MAPK pathway rather than PI3K pathway.

Rezai *et al.* (Rezai *et al.*, 1997) showed that the POS phagocytic capacity of IPE cells was 70% of RPE cells. We also reported that phagocytic activity was promoted in IPE cells by using a transferred bFGF cDNA gene (Sakuragi *et al.*, 2001). However, the mechanisms of IPE phagocytosis are not well understood. In the present study, we showed that the addition of POS immediately phosphorylated ERK1/2 but not Akt. It is possible that the phosphorylation of ERK1/2 plays an important role in the phagocytic process. It has been reported that ERKs were highly activated during the phagocytic process in polymorphonuclear leukocytes (Suchard *et al.*, 1997). The phosphorylation of ERKs is a key factor during the phagocytic process in other cell types such as macrophages (Ibata-Ombetta *et al.*, 2001) and leukocytes (Suchard *et al.*, 1997). In contrast, it is reported that the PI3K pathway plays an important role in actin assembly, pseudopod extension and phagosomal closure in macropharges during phagocytosis (Araki *et al.*, 1996; Cox *et al.*, 1999). Interestingly, it was reported that the pathway of phagocytosis changed depending on the phase of phagocytosis, for example, from ERK dependent in early phase to ERK and PI3K dependent in late phase (Garcia-Garcia *et al.*, 2002).

It has been thought that the phagocytic process of POS in RPE cells was a non-inflammatory clearance and involved a different type of phagocytosis with macrophages (Edwards and Szamier, 1977; Hall, 1978; Mayerson and Hall, 1986). Therefore we cannot simply adhere to the phagocytic process of IPE cells. In our data, BDNF markedly increased the phosphorylation of ERK1/2 while PD98059 inhibited increased binding of POS and the decreased ingestion of POS. However, the fact that the inhibition of the binding by PD98059 was up to control level and the binding of POS in control IPE cells was not affected by PD98059 (Fig. 2B, C), indicated that another pathway exists in normal binding processes. Interestingly, the ingestion of POS in control IPE cells was also inhibited by PD98059 though PD98059 was not affected by the POS binding process in control IPE cells. We previously reported that a cathepsin S activity, which is related to the POS digestion, rapidly activated within three hours after the POS application (Sugano *et al.*, 2006). Taken together, PD98059 might have some effect on

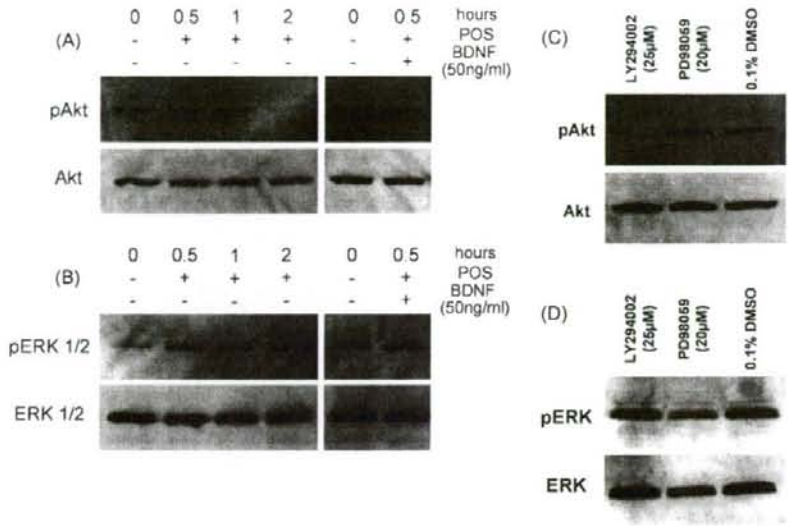

Fig. 3. Western blot analysis of cell lysates for phosphorylated Akt (A) or ERKs (B) after the addition of POS or BDNF. LY294002 completely inhibited the phosphorylation of Akt (C). Phosphorylated ERKs were partially inhibited by the addition of PD98059 (D).

their digestive process including activations of digestive enzymes such as cathepsins of the ingested POS. The details of these mechanisms, however, are not clear at the present time.

The MAPK pathway is involved in many physiological events. Many reports have been published regarding the correlation of MAPK and cell proliferation (Hecquet *et al.*, 2002; King *et al.*, 2005; Liou *et al.*, 2002). We previously reported that PD98059 inhibits rat RPE cell replication by cell cycle arrest (Yamaguchi *et al.*, 2002), and observed that high phagocytic activity in RPE cells was in the proliferative phase (unpublished data). Increased phagocytic activity by BDNF might be related to cell cycles of IPE cells. Further studies are needed to confirm effects of phagocytic activities *in vivo*. Our final goal is to protect photoreceptor cells by the subretinal transplantation of iris pigment epithelial (IPE) cells transduced by using a BDNF gene (Hojo *et al.*, 2004). Changes in phagocytic activities reported here might provide keys to our final goal.

Acknowledgement. This work was supported in part by Grants-in-Aid for Scientific Research from the Ministry of Education Science and Culture (No. 17390465, 17791217, 17659541), Special Coordination Funds for Promoting Science and Technology of the Japanese Government, Japanese Retinitis Pigmentosa Society, and The Suzuken Memorial Foundation. We thank Mr. Jon Sorensen and Mrs. Kimberly Sorensen for assistance with manuscript preparation.

References

Abe, T., Tomita, H., Kano, T., Yoshida, M., Ohashi, T., Nakamura, Y., Nishikawa, S., and Tamai, M. 2000a. Autologous iris pigment epithelial cell transplantation in monkey subretinal region. *Curr. Eye Res.*, **20**: 268–275.

Abe, T., Tomita, H., Ohashi, T., Yamada, K., Takeda, Y., Akaishi, K., Yoshida, M., Sato, M., and Tamai, M. 1999a. Characterization of iris pigment epithelial cell for auto cell transplantation. *Cell Transplant.*, **8**: 501–510.

Abe, T., Yoshida, M., Tomita, H., Kano, T., Nakagawa, Y., Sato, M., Wada, Y., Fuse, N., Yamada, T., and Tamai, M. 1999b. Functional analysis after auto iris pigment epithelial cell transplantation in patients with age-related macular degeneration. *Tohoku J. Exp. Med.*, **189**: 295–305.

Abe, T., Yoshida, M., Tomita, H., Kano, T., Sato, M., Wada, Y., Fuse, N., Yamada, T., and Tamai, M. 2000b. Auto iris pigment epithelial cell transplantation in patients with age-related macular degeneration: short-term results. *Tohoku J. Exp. Med.*, **191**: 7–20.

Araki, N., Johnson, M.T., and Swanson, J.A. 1996. A role for phosphoinositide 3-kinase in the completion of macropinocytosis and phagocytosis by macrophages. *J. Cell Biol.*, **135**: 1249–1260.

Barnabe-Heider, F. and Miller, F.D. 2003. Endogenously produced neurotrophins regulate survival and differentiation of cortical progenitors via distinct signaling pathways. *J. Neurosci.*, **23**: 5149–5160.

Bok, D. and Hall, M.O. 1971. The role of the pigment epithelium in the etiology of inherited retinal dystrophy in the rat. *J. Cell Biol.*, **49**: 664–682.

Chaitin, M.H. and Hall, M.O. 1983. Defective ingestion of rod outer segments by cultured dystrophic rat pigment epithelial cells. *Invest. Ophthalmol. Vis. Sci.*, **24**: 812–820.

Cox, D., Tseng, C.C., Bjekic, G., and Greenberg, S. 1999. A requirement for phosphatidylinositol 3-kinase in pseudopod extension. *J. Biol. Chem.*, **274**: 1240–1247.

Edwards, R.B. and Szamier, R.B. 1977. Defective phagocytosis of isolated

rod outer segments by RCS rat retinal pigment epithelium in culture. *Science*, **197**: 1001–1003.

Feng, W., Yasumura, D., Matthes, M.T., LaVail, M.M., and Vollrath, D. 2002. Mertk triggers uptake of photoreceptor outer segments during phagocytosis by cultured retinal pigment epithelial cells. *J. Biol. Chem.*, **277**: 17016–17022.

Fryer, H.J., Wolf, D.H., Knox, R.J., Strittmatter, S.M., Pennica, D., O'Leary, R.M., Russell, D.S., and Kalb, R.G. 2000. Brain-derived neurotrophic factor induces excitotoxic sensitivity in cultured embryonic rat spinal motor neurons through activation of the phosphatidylinositol 3-kinase pathway. *J. Neurochem.*, **74**: 582–595.

Garcia-Garcia, E., Rosales, R., and Rosales, C. 2002. Phosphatidylinositol 3-kinase and extracellular signal-regulated kinase are recruited for Fc receptor-mediated phagocytosis during monocyte-to-macrophage differentiation. *J. Leukoc. Biol.*, **72**: 107–114.

Hall, M.O. 1978. Phagocytosis of light- and dark-adapted rod outer segments by cultured pigment epithelium. *Science*, **202**: 526–528.

Hans, A., Bajramovic, J.J., Syan, S., Perret, E., Dunia, I., Brahic, M., and Gonzalez-Dunia, D. 2004. Persistent, noncytolytic infection of neurons by Borna disease virus interferes with ERK 1/2 signaling and abrogates BDNF-induced synaptogenesis. *FASEB J.*, **18**: 863–865.

Hecquet, C., Lefevre, G., Valtink, M., Engelmann, K., and Mascarelli, F. 2002. Activation and role of MAP kinase-dependent pathways in retinal pigment epithelial cells: ERK and RPE cell proliferation. *Invest. Ophthalmol. Vis. Sci.*, **43**: 3091–3098.

Herron, W.L., Riegel, B.W., Myers, O.E., and Rubin, M.L. 1969. Retinal dystrophy in the rat—a pigment epithelial disease. *Invest. Ophthalmol.*, **8**: 595–604.

Hojo, M., Abe, T., Sugano, E., Yoshioka, Y., Saigo, Y., Tomita, H., Wakusawa, R., and Tamai, M. 2004. Photoreceptor protection by iris pigment epithelial transplantation transduced with AAV-mediated brain-derived neurotrophic factor gene. *Invest. Ophthalmol. Vis. Sci.*, **45**: 3721–3726.

Ibata-Ombetta, S., Jouault, T., Trinel, P.A., and Poulain, D. 2001. Role of extracellular signal-regulated protein kinase cascade in macrophage killing of Candida albicans. *J. Leukoc. Biol.*, **70**: 149–154.

Kano, T., Abe, T., Tomita, H., Sakata, T., Ishiguro, S., and Tamai, M. 2002. Protective effect against ischemia and light damage of iris pigment epithelial cells transfected with the BDNF gene. *Invest. Ophthalmol. Vis. Sci.*, **43**: 3744–3753.

Kelly-Spratt, K.S., Klesse, L.J., Merenmies, J., and Parada, L.F. 1999. A TrkB/insulin receptor-related receptor chimeric receptor induces PC12 cell differentiation and exhibits prolonged activation of mitogen-activated protein kinase. *Cell Growth Differ.*, **10**: 805–812.

King, R.E., Kent, K.D., and Bomser, J.A. 2005. Resveratrol reduces oxidation and proliferation of human retinal pigment epithelial cells via extracellular signal-regulated kinase inhibition. *Chem. Biol. Interact.*, **151**: 143–149.

LaVail, M.M. and Battelle, B.A. 1975. Influence of eye pigmentation and light deprivation on inherited retinal dystrophy in the rat. *Exp. Eye Res.*, **21**: 167–192.

LaVail, M.M., Unoki, K., Yasumura, D., Matthes, M.T., Yancopoulos, G.D., and Steinberg, R.H. 1992. Multiple growth factors, cytokines, and neurotrophins rescue photoreceptors from the damaging effects of constant light. *Proc. Natl. Acad. Sci. USA*, **89**: 11249–11253.

Lindsay, R.M. 1994. Trophic protection of motor neurons: clinical potential in motor neuron diseases. *J. Neurol.*, **242**: S8–11.

Liou, G.I., Pakalnis, V.A., Matragoon, S., Samuel, S., Behzadian, M.A., Baker, J., Khalil, I.E., Roon, P., Caldwell, R.B., Hunt, R.C., and Marcus, D.M. 2002. HGF regulation of RPE proliferation in an IL-1beta/retinal hole-induced rabbit model of PVR. *Mol. Vis.*, **8**: 494–501.

Mayerson, P.L. and Hall, M.O. 1986. Rat retinal pigment epithelial cells show specificity of phagocytosis in vitro. *J. Cell Biol.*, **103**: 299–308.

Nakazawa, T., Tamai, M., and Mori, N. 2002. Brain-derived neurotrophic factor prevents axotomized retinal ganglion cell death through MAPK and PI3K signaling pathways. *Invest. Ophthalmol. Vis. Sci.*, **43**: 3319–3326.

Papermaster, D.S. and Dreyer, W.J. 1974. Rhodopsin content in the outer segment membranes of bovine and frog retinal rods. *Biochemistry*, **13**: 2438–2444.

Peinado-Ramon, P., Salvador, M., Villegas-Perez, M.P., and Vidal-Sanz, M. 1996. Effects of axotomy and intraocular administration of NT-4, NT-3, and brain-derived neurotrophic factor on the survival of adult rat retinal ganglion cells. A quantitative *in vivo* study. *Invest. Ophthalmol. Vis. Sci.*, **37**: 489–500.

Rezai, K.A., Lappas, A., Farrokh-siar, L., Kohen, L., Wiedemann, P., and Heimann, K. 1997. Iris pigment epithelial cells of long evans rats demonstrate phagocytic activity. *Exp. Eye Res.*, **65**: 23–29.

Rocha, M., Martins, R.A., and Linden, R. 1999. Activation of NMDA receptors protects against glutamate neurotoxicity in the retina: evidence for the involvement of neurotrophins. *Brain Res.*, **827**: 79–92.

Sakuragi, M., Tomita, H., Abe, T., and Tamai, M. 2001. Changes of phagocytic capacity in basic fibroblast growth factor-transfected iris pigment epithelial cells in rats. *Curr. Eye Res.*, **23**: 185–191.

Soppet, D., Escandon, E., Maragos, J., Middlemas, D.S., Reid, S.W., Blair, J., Burton, L.E., Stanton, B.R., Kaplan, D.R., Hunter, T. *et al.* 1991. The neurotrophic factors brain-derived neurotrophic factor and neurotrophin-3 are ligands for the trkB tyrosine kinase receptor. *Cell*, **65**: 895–903.

Suchard, S.J., Mansfield, P.J., Boxer, L.A., and Shayman, J.A. 1997. Mitogen-activated protein kinase activation during IgG-dependent phagocytosis in human neutrophils: inhibition by ceramide. *J. Immunol.*, **158**: 4961–4967.

Sugano, E., Tomita, H., shiguro, S., Isago, H., and Tamai, M. 2006. Nitric oxide-induced accumulation of lipofuscin-like materials is caused by inhibition of cathepsin S. *Curr. Eye Res.*, **31**: 607–616.

Tomita, H., Ishiguro, S., Abe, T., and Tamai, M. 1999. Administration of nerve growth factor, brain-derived neurotrophic factor and insulin-like growth factor-II protects phosphate-activated glutaminase in the ischemic and reperfused rat retinas. *Tohoku J. Exp. Med.*, **187**: 227–236.

Unoki, K. and LaVail, M.M. 1994. Protection of the rat retina from ischemic injury by brain-derived neurotrophic factor, ciliary neurotrophic factor, and basic fibroblast growth factor. *Invest. Ophthalmol. Vis. Sci.*, **35**: 907–915.

Watanabe, M., Sawai, H., and Fukuda, Y. 1997. Survival of axotomized retinal ganglion cells in adult mammals. *Clin. Neurosci.*, **4**: 233–239.

Yamaguchi, K., Tomita, H., Sugano, E., Nakazawa, T., and Tamai, M. 2002. Mitogen-activated protein kinase inhibitor, PD98059, inhibits rat retinal pigment epithelial cell replication by cell cycle arrest. *Jpn. J. Ophthalmol.*, **46**: 634–639.

Young, R.W. 1967. The renewal of photoreceptor cell outer segments. *J. Cell Biol.*, **33**: 61–72.

Young, R.W. and Bok, D. 1969. Participation of the retinal pigment epithelium in the rod outer segment renewal process. *J. Cell Biol.*, **42**: 392–403.

(Received for publication, July 19, 2007 and accepted, February 4, 2008)

Reprod Dom Anim **43**, 66–73 (2008); doi: 10.1111/j.1439-0531.2007.00856.x
ISSN 0936-6768

Morphometric and Ultrastructural Changes in Ciliated Cells of the Oviductal Epithelium in Prolific Chinese Meishan and Large White Pigs during the Oestrous Cycle

H Abe[1] and H Hoshi[2]

[1]*Tohoku University Biomedical Engineering Research Organization (TUBERO), Sendai, Japan;* [2]*Research Institute for the Functional Peptides, Yamagata, Japan*

Contents

There are some differences in reproductive features between the Chinese Meishan (CM) pig and Large White (LW) pig. The aim of the present study was to investigate the quantitative changes and ultrastructural features of ciliated cells in the various regions of the CM and LW pig oviduct during the follicular and luteal phases of the oestrous cycle. In the fimbrial and ampullar epithelia at the follicular phase, the ciliated cells were more plentiful than in the isthmic region in both pigs. In the CM pigs, there was a striking decrease in the percentage and cell height of ciliated cells in the luteal phase compared with the follicular phase. Although similar quantitative changes were observed in the LW pig oviduct, these changes were less dramatic than that in the CM pig oviduct. In both pigs, the percentage and cell height of ciliated cells in the isthmus were unchanged between the follicular and luteal phases. The ultrastructure of ciliogenic and ciliated cells was observed. In the fimbrial and ampullar epithelia during the follicular phase, most of the ciliated cells showed normal morphology, having many elongated cilia and mitochondria, but in the CM pig oviduct during the luteal phase many of the ciliated cells possessed immature cilia and swollen mitochondria. Cells undergoing ciliogenesis were frequently observed in the fimbriae and ampulla, and occasionally in the isthmus. Cytoplasmic protrusions containing variable numbers of ciliary axonemal complexes occurred in the fimbrial and ampullar epithelium in the CM pigs at the luteal phase, suggesting that deciliation of cells occurs by membrane-bound cilia packets forming at the apices of cells and pinching off. These results demonstrate that there are regional variations in the cyclic changes associated with the oviductal ciliated cells of the pigs, while there are marked morphometrical and ultrastructural changes in oviductal ciliated cells of the CM pigs compared with that of the LW pigs.

Introduction

The epithelium of the oviduct consists of two types of cell: ciliated and nonciliated secretory cells. The ciliated cells may play an important role in the transport of oocytes and embryos (Odor and Blandau 1973) and possibly in the regulation of sperm progression (Hunter et al. 1991). On the other hand, the secretory cells produce and release specific secretory materials which may play important roles in embryonic development and sperm function (Hunter 1994; Abe et al. 1995; Gandolfi 1995). These cells undergo marked morphological and functional changes in association with fluctuations of the ovarian hormones during the oestrous cycle (Rumery et al. 1978; Odor et al. 1980). Moreover, it is known that the oviductal epithelial cells show marked regional variations in ultrastructural, histochemical, biochemical, and physiological features in many mammals (Abe 1996).

The Chinese Meishan (CM) pig is known as a precocious and prolific breed (Cheng 1984). It has been reported that there are differences in rates of ovulation, embryo-placental development, and the size of the uterus between the Large White (LW) pig and the CM pig (Bazer et al. 1988a,b). In particular, it seems that the reproduction success of the CM pig is associated with higher rates of embryo development. Therefore, it is of great interest to compare the ultrastructural features of oviductal epithelial cells between the CM pig and the LM pig. In previous studies, it has been described the ultrastructural features of epithelial cells in the LW pig oviduct (Nayak et al. 1976a,b, 1976c, 1977). The surface morphology of oviductal epithelium has been investigated in LW pigs (Stalheim et al. 1975; Wu et al. 1976; Yaniz et al. 2006). Similarly, the luminal surfaces of epithelial cells in various regions of the oviducts of CM pigs were examined by scanning electron microscopy (Abe and Oikawa 1992). However, available information on the reproductive tracts, including the oviduct of CM pig, is still limited.

Recently, we have reported the marked regional changes in the ultrastructural features of secretory cells in the CM pig oviduct, which are associated with the stages of the oestrous cycle (Abe and Hoshi 2007). This study provides insight into the regional and cellular differences in functions of secretory cells of the CM pig oviduct. Therefore, it is important to investigate how cytomorphometric and ultrastructural changes of ciliated cells occur in the CM pig oviduct during the oestrous cycle. The objective of the current study was to: (i) quantitate the numbers and heights of ciliated cells, (ii) examine the ultrastructure of the ciliogenic and ciliated cells present in the fimbrial, ampullar, and isthmic epithelium of the oviduct at the follicular and luteal phase of the oestrous cycle and (iii) compare these morphological features between the CM pig and the LW pig.

Materials and Methods

Sexually mature CM pigs and LW pigs were observed at least twice per day for evidence of oestrus before they were placed into an experiment. Two groups of three CM pigs and five LM pigs at different stages of the oestrous cycle (day 1 and days 10–14) were killed at a local meat processing plant. Day 1 refers to the day of

onset of oestrus (follicular phase), and days 10–14 refer to the late dioestrus (luteal phase). The stages of the cycle were confirmed by careful examination of the ovaries according to the previous method (Akins and Morrissette 1968). They were destinated to the food chain after slaughter.

Oviductal segments were processed for transmission electron microscopy according to our previous study (Abe and Oikawa 1992). Oviducts were recovered within 20 min of slaughter. After the oviduct had been trimmed of fat and extraneous tissue, the fimbriae, ampulla, and isthmus were cut apart. Strips of tissue were cut along the borders of the fimbrial folds and the luminal ridges of the ampulla and isthmus. These tissues were fixed by immersion in 2% paraformaldehyde (PA)-2.5% glutaraldehyde (GA) for 3 h. After fixation, the segments were trimmed into small pieces and fixed again for 3 h in 2% PA-2.5% GA. The pieces of tissue were postfixed for 2 h with 1% osmium tetroxide. All fixatives were prepared in 0.1 M phosphate buffer (pH 7.4) and tissues were rinsed after fixation in phosphate buffer. All fixation and rinsing steps were carried out at 0–4°C. Osmolality of PA-GA fixative was approximately 400 mOsm. After fixation, the oviducts were dehydrated in ascending concentrations of ethanol, and embedded in Epon 812 resin (Taab Laboratories Equipment Ltd, Berkshire, UK). All sections were prepared using an ultramicrotome (NOVA, Pharmacia LKB, Uppsala, Sweden). Semithin sections were cut with a glass knife and ultrathin sections were cut with a diamond knife. Semithin sections were placed on glass slides, stained with 1% toluidine blue and examined under a light microscope (BH2: Olympus Optical Co., Ltd, Tokyo, Japan). Ultrathin sections were stained with uranyl acetate and lead citrate and examined using a transmission electron microscope (JEM-100SX, Jeol, Tokyo, Japan) operated at 60 kV.

To obtain quantitative data on the percentage of ciliated cells, 1.5 μm semithin sections of cells were examined under the light microscope as in the method described previously (Abe and Oikawa 1992). The percentages of ciliated cells were determined by scanning 250–500 cells per block from at least three different blocks of fimbriae, ampulla, and isthmus per animal. All the epithelial cells that extended as far as the luminal surface were counted, while those in obliquely cut areas were excluded. The height of epithelial cells and the length of cilia were measured with an ocular micrometer. For these measurements we selected, in each region, 75–125 ciliated cells in which the plane of the section clearly passed through the cell nucleus, parallel to the longitudinal axis of the cell. Each result is expressed as the mean ± standard error of the mean.

Statistical analyses were performed using one-way analysis of variance (ANOVA, Abacus Concepts, StatView, Berkeley, CA, USA) and Fisher's protected least significant differences test.

Results

Figure 1 shows the morphology of the mucosa in the three regions of CM pig oviduct during both the follicular and luteal phases of the oestrous cycle. In the epithelium of all regions, two distinct cell types, ciliated and nonciliated (secretory) cells were distinguished. During the follicular phase, ciliated cells were predominate in the fimbrial epithelium (Fig. 1a). Basophilic granules were present in the apical cytoplasm of

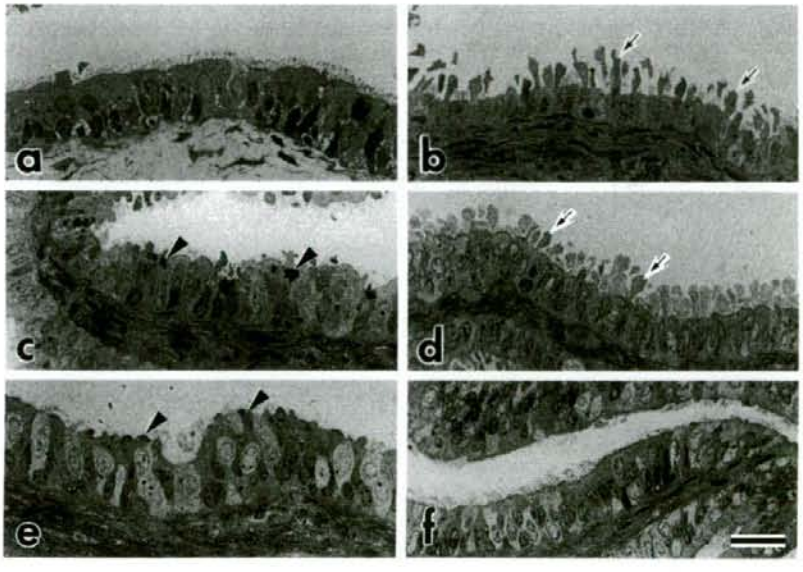

Fig. 1. Light micrographs of Chinese Meishan pig oviduct in cross-section showing the fimbriae (a, b), ampulla (c, d), and isthmus (e, f). (a, c, e) Follicular phase. (b, d, f) Luteal phase. Basophilic granules (arrowheads) are found in nonciliated cells in the ampulla (c) and isthmus (e) in the follicular phase. The cells are extended from the epithelium (arrows in b,d) in the luteal phase. Bar 20 μm

nonciliated cells in the ampulla and isthmus in the follicular phase (Fig. 1c, e). The apices of nonciliated cells showed various degree of protrusion. The protrusions extended beyond the tips of the cilia in the epithelium of the fimbriae (Fig. 1b) and ampulla (Fig. 1d) in the luteal phase. The epithelium of all oviductal regions in LW pig appeared similar to that in CM pig (not shown).

Figure 2 shows the mean percentage of ciliated cells and the cell height of ciliated and nonciliated cells in the oviductal epithelium of the fimbriae, ampulla, and isthmus during the follicular and luteal phases of the oestrous cycle. In CM pig, the mean percentage of ciliated cells significantly decreased from 81.1% in the fimbriae and 61.2% in the ampulla in the follicular phase to 31.0% and 39.7%, respectively in the luteal phase (Fig. 2a). Although the mean percentage of ciliated cells in LW pig oviduct significantly decreased from 80.5% in the fimbriae in the follicular phase to 74.7% in the luteal phase, this reduction was less dramatic than that in CM pig oviduct. The percentage of ciliated cells in the ampulla of LW pig oviduct was not significantly different between the follicular and luteal phases, 61.2% and 61.9%, respectively. In the isthmus, the drastic changes in percentage of ciliated cells were not observed between the follicular and luteal phases (34.0% and 34.4% in CM pig; 35.0% and 38.7% in LW pig, respectively). In both pigs, the height (μm) of ciliated cells in the epithelium of fimbrial and ampullar regions was dramatically reduced in the luteal phase compared with the follicular phase (follicular vs luteal: 29.7 vs 15.7 in fimbriae and 27.9 vs 16.4 in ampulla in CM pig; 30.3 vs 18.4 in fimbriae and 31.7 vs 17.4 in ampulla in LW pig, respectively) (Fig. 2b). The height of nonciliated cells was reduced in the epithelium in these two regions, although the reductions were less dramatic than those in the ciliated cells (follicular vs luteal: 32.7 vs 26.8 in fimbriae and 29.5 vs 25.6 in ampulla in CM pig; 30.5 vs 25.6 in fimbriae and 32.5 vs 24.8 in ampulla in LW pig, respectively) (Fig. 2c). In the isthmus, there are no marked changes in the height of ciliated (follicular vs luteal: 28.0 vs 26.8 in CM pig; 29.3 vs 27.7 in LW pig, respectively) and nonciliated (follicular vs luteal: 30.4 vs 28.3 in CM pig; 30.2 vs 28.8 in LW pig, respectively).

In the fimbrial epithelium of CM pig oviduct in the follicular phase, the ciliated cells contained indented nuclei composed primarily of euchromatin and distinct nucleoli (Fig. 1a, 3a). The mature ciliated cells were characterized by cilia, basal bodies, and an apical distribution of numerous mitochondria. Many of the mitochondria were long and oriented parallel to the long axis of the cell (Fig. 3b). Numerous polysomal complexes were scattered throughout the cytoplasm. Many mature cilia protruded at the apical surface of the ciliated cells. The ultrastructural features of mature ciliated did not differ between CM and LW pigs.

During the luteal phase, some marked changes in ultrastructural features were observed in the ciliated cells of the fimbrial region in the MS pig oviduct. In general, most ciliated cells had low electron density cytoplasm compared with that of the nonciliated cells (Fig. 3c). The nuclei of many cells showed ovoid structures and were composed of more prominent

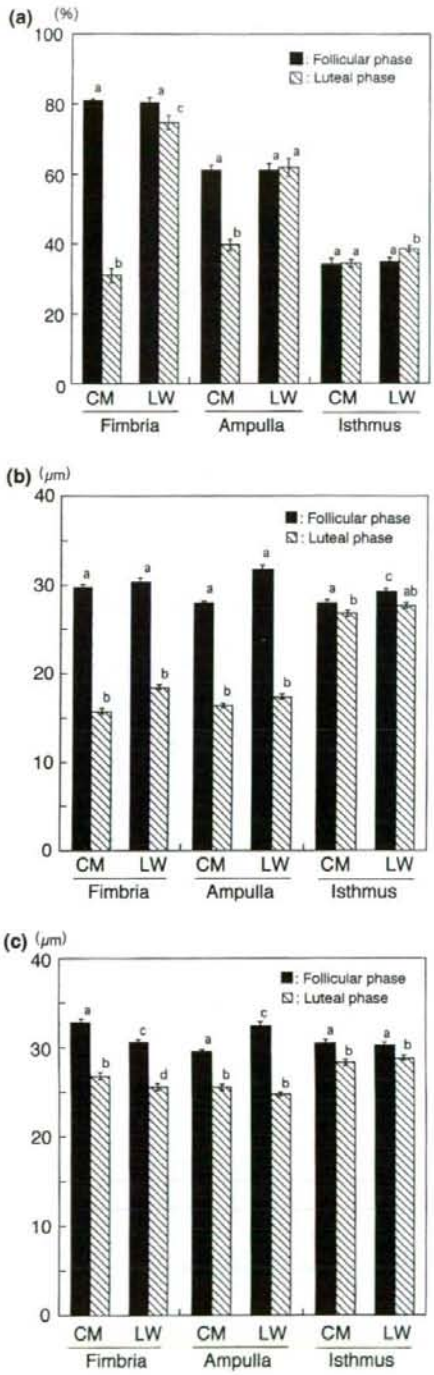

Fig. 2. Cyclic and segmental variations in proportion (a) and cell height of ciliated cells (b) and nonciliated cells (c) in the epithelium at the fimbrial, ampullar, and isthmic regions of the Chinese Meishan (CM) and Large White (LW) pig oviducts. Values are expressed as mean ± SEM (proportion: n = 9, cell height: n = 79–125). Values with different superscripts in each column (oviductal segment) differ significantly ($p < 0.05$)

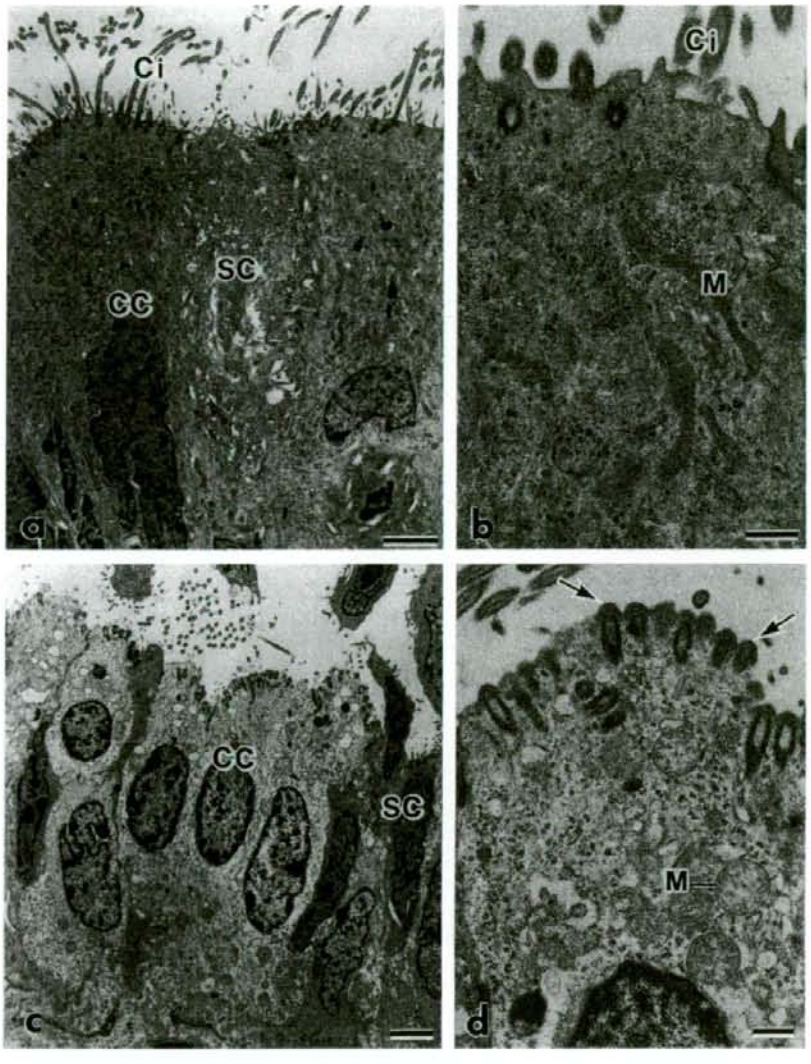

Fig. 3. Fimbrial epithelial cells of Chinese Meishan pig oviducts at follicular (a, b) and luteal (c, d) phases of the oestrous cycle. (a, b) The fimbrial ciliated cells have many mature cilia (Ci) and elongated mitochondria (M). (c, d) During the luteal phase, ciliated cells (CC) have low electron-dense cytoplasm and many short cilia (arrows). Many swollen mitochondria are seen in the supranuclear cytoplasm. BL, basal lamina; SC, secretory cells. Bars a, c = 2 μm; b, d = 0.5 μm

heterochromatin at the peripheral margins of the nuclear membrane compared with the follicular phase. The cilia were shorter than those in the follicular phase and these immature cilia had a characteristic blunt tip (Fig. 3d). Most mitochondria had a round shape. In the ampulla and isthmus, the mature ciliated cells showed similar ultrastructural features to the fimbrial ciliated cells. These ciliated cells possessed a nucleus with nucleoli and condensed chromatin, cilia, basal bodies, and elongated mitochondria, and there were no dramatic ultrastructural changes as were observed in the fimbriae during the luteal phase (not shown).

Cells demonstrating ciliogenesis were observed with moderate frequency in the epithelium of the fimbriae and occasionally in the ampulla and isthmus. The frequency of appearance of ciliogenic cells was higher in the follicular phase than in the luteal phase. In these ciliogenic cells, many fibrous granules, which were small and round, and electron-dense granules without a limiting membrane, were observed in the area between the nucleus and the apex of cell (Fig. 4a). Also, several deuterosomes, which were of higher electron density than the fibrous granules, occurred near aggregates of the fibrous granules. The deuterosomes were classified into two types. One type appeared spherical and solid, 0.1–0.2 μm in diameter, while the other appeared hollow, and 0.2–0.5 μm in diameter (Fig. 4a, inset). Procentrioles arose around the deuterosomes in

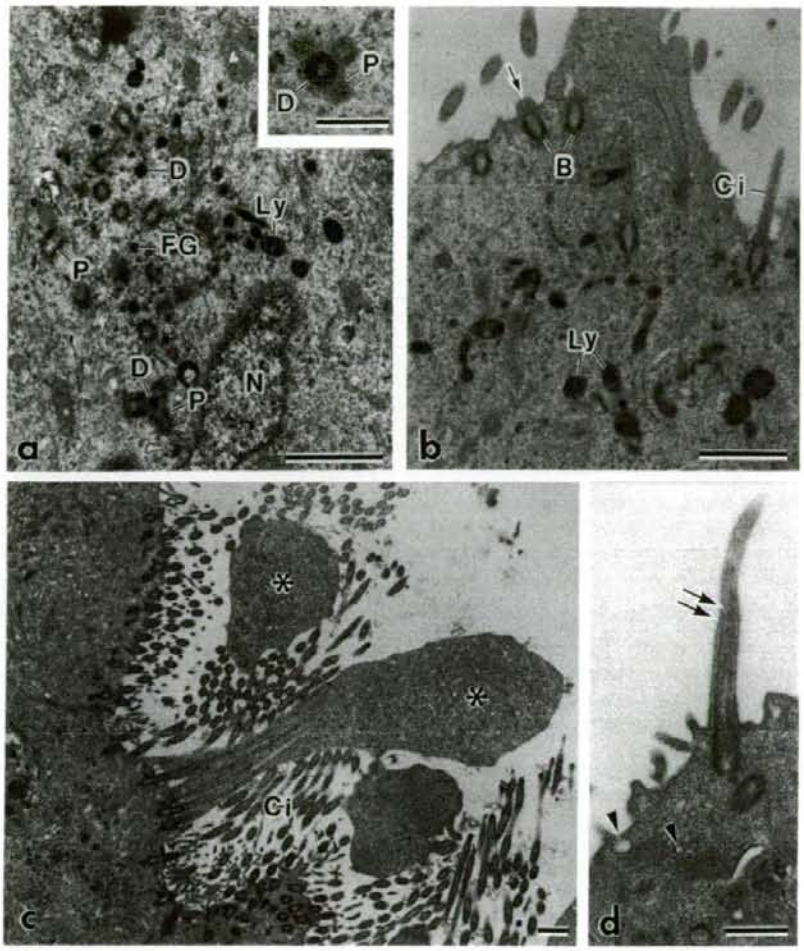

Fig. 4. Apical portions of epithelial cells of the Chinese Meishan pig oviduct. (a, b) Ciliogenic cells. Aggregates of fibrous granules (FG) around deuterosomes (D) are seen in the supranuclear cytoplasm. The insertion illustrates a hollow deuterosome. Procentrioles (P) are located around the deuterosome in a spoke-like arrangement. Some lysosome-like bodies (Ly) are seen around the deuterosome and procentrioles. Basal bodies (B) are forming cilia and small bulge (arrow) in the cell membrane is seen (arrow). (c) Ciliated cells of the fimbrial epithelium. Cytoplasmic protrusions (asterisks) contain internalized parts of ciliary axonemes. (d) An epithelial cell illustrating the presence of a solitary cilium (SC). Notice the small endocytotic vesicles (arrowheads). Bars a, b, c = 1 μm; d, Inset in a = 0.5 μm

a spoke-like formation and developed into basal bodies. Usually, one deuterosome was associated with one to six procentrioles. The basal bodies migrated from near the aggregates of fibrous granules to the apical surface of the cell and there initiated the formation of cilia (Fig. 4b). As a result, ciliary buds were formed and each of them induced formation of a small bulge in the cell membrane, which eventually induced elongation of the cell membrane around the developing cilium. Sometimes, an irregular cytoplasmic process surrounding the elongating cilium was observed. In the fimbrial epithelium, irregular cytoplasmic protrusions were frequently observed in the mature ciliated cells at the luteal phase. Most of the protrusions were free of cellular organelles but contained internalized parts of ciliary axonemes (Fig. 4c). In some cells, a solitary cilium projected into the lumen and small vesicles that appeared to be endocytotic vesicle were observed in the apical cytoplasm (Fig. 4d).

Discussion

This study demonstrates that the oviductal epithelium of the CM pig and LM pig undergoes a drastic change in ciliation during the oestrous cycle. Large numbers of ciliated cells were present in the epithelium of fimbriae and ampulla during the follicular phase, while the numbers of ciliated cells was significantly reduced in the luteal phase. Moreover, the height of the ciliated cells decreased noticeably in the luteal phase. These changes were particularly dramatic in the fimbriae. Similar observations have been described in the oviduct of the domestic animals (Abe and Oikawa 1993b; Abe et al. 1993). Cilia are thought to be primarily responsible for

the pickup and transport of ovulated eggs in the fimbriae, and the cilia of the ampullar epithelium have a similar function (Odor and Blandau 1973). A richly ciliated epithelium at ovulation (follicular stage) is important. It seems that the cyclic changes observed in the present study reflect the function of the cilia in the fimbriae and ampulla of the pig oviduct.

In the present cytomorphometric study, the numbers of ciliated cells in the pig oviductal epithelium, especially in the CM pig oviduct, significantly decreased in the fimbrial and ampullar regions at the luteal phase. Similar changes in ciliation have been observed in the primate oviducts (Rumery et al. 1978; Odor et al. 1980; Brenner et al. 1983). In the oviduct of the rhesus monkey, Brenner (1969a,b) demonstrated that large numbers of cilia are formed during the follicular phase, creating a richly ciliated epithelium, and extensive atrophy and deciliation take place during the luteal phase of the menstrual cycle. Deciliation is associated with a 'pinching off' of the apical portion of each ciliated cell (Brenner 1969a). Similar findings have been described in the oviduct of the pig-tailed monkey (Odor et al. 1980). In our previous study using scanning electron microscopy, 'pinching off' of the apical portions of epithelial cells was frequently observed in the CM pig oviduct (Abe and Oikawa 1992). The present study demonstrated that these apical protrusions contained internalized parts of ciliary axonemes. These findings suggest that the reduction in number of ciliated cells in the luteal phase may be accomplished by shedding of the cilia into the oviductal lumen.

The cells showing ciliogenesis were found in the fimbrial and ampulla epithelia during the oestrous cycle. The ultrastructural features of ciliogenesis observed in the CM pig oviductal epithelium were similar to those described in the oviducts of other species (Anderson and Brenner 1971; Dirksen 1971; McCarron and Anderson 1973; Komatsu and Fujita 1978b; Abe and Oikawa 1989). The initial event in ciliogenesis is the appearance of fibrous granules in the apical cytoplasm of the future ciliated cells. These fibrous granules are also called proliferative elements (Dirksen and Crocker 1965) and procentriole precursors or axonemal precursors (Steinman 1968). The second event in ciliogenesis is the appearance of electron-dense spherical bodies, designated deuterosomes (Sorokin 1968), within the aggregation of fibrous granules. The procentrioles begin to form shortly after or simultaneously with the appearance of fibrous granules and deuterosomes, and each procentriole usually develops in contact with the deuterosomes. Eventually, procentrioles lengthen, break away from the deuterosome, migrate toward the cell surface, and then each centriole becomes associated with the cell membrane to form a ciliary bud, which grows into a cilium. In the ciliogenic cells present in the oviductal epithelium of the CM pig, the deuterosomes were distinguished into two types, solid and hollow. The hollow type has never been observed in the monkey oviduct (Anderson and Brenner 1971), but both solid and hollow deuterosomes have been seen in the oviduct of the mouse (Komatsu and Fujita 1978a) and golden hamster (Abe and Oikawa 1989). It is not clear whether deuterosomes are actually utilized in the formation of the procentriole or whether they act merely as organizers for the generation of the procentriole.

The ciliated cells of the isthmus showed few changes between the follicular and luteal phases, in contrast to those of the fimbriae and ampulla. It has been suggested that the isthmic epithelial cells act as a sperm reservoir (Hunter et al. 1991). That study demonstrated specific and active interactions between the tips of the cilia and the flagella of bull spermatozoa in the caudal isthmus of the oviduct of cows, suggesting that the cilia in the oviductal isthmus may regulate contacts with spermatozoa flagella. In addition, some studies suggest that isthmic epithelial cells may have the ability to maintain the viability and fertilizing capacity of spermatozoa (Smith et al. 1987; Pollard et al. 1991; Suarez et al. 1991). However, the main function of isthmic ciliated cells of the mammalian oviduct remains unresolved.

The cytomorphometric analysis and transmission electron microscopy data of the present study revealed that there were marked regional differences in epithelial cells of the pig oviduct during cyclic changes. Although the reason for the regional differences is unclear, these regional differences may reflect regional variations in sensitivity to ovarian steroid hormones. Many studies have demonstrated that cytodifferentiation of epithelial cells of the oviduct is closely related to the effects of ovarian steroid hormones (Brenner et al. 1974; Verhage and Brenner 1975; Odor et al. 1980; Abe and Oikawa 1993a). In addition, it has been suggested that the regular cycle of ciliogenesis and deciliation by the epithelial cells of the mammalian oviduct is dependent upon the levels of circulating estrogen and progesterone (Brenner et al. 1974; Verhage et al. 1979; Abughrien and Dore 2000). Ciliogenesis in the follicular phase occurs under the influence of estrogen, while the appearance of progesterone at midcycle suppresses ciliogenesis and leads to deciliation. Moreover, it has been suggested by others that oviductal epithelial cells show regional differences in their responses to steroid hormones (Gupta et al. 1969; Fredricsson and Holm 1974; Bajpai et al. 1977). These findings strongly support our hypothesis that there are regional differences in the responses to hormones of epithelial cells in the various regions of the Chinese Meishan pig oviduct.

A solitary or single cilium, also designated a rudimentary or temporary cilium, was frequently observed in the CM pig oviductal epithelial cells in the luteal phase. Odor and Blandau (1985) observed such solitary cilia more frequently in the oviductal epithelium of ovariectomized and ovariectomized/progesterone-treated rabbits than in controls. Also, solitary cilia have been found on undifferentiated epithelial cells of neonatal oviducts (Komatsu and Fujita 1978a; Odor and Blandau 1985; Abe and Oikawa 1989). These findings suggest that the appearance of solitary cilia may be closely related to fluctuations in levels of ovarian hormones.

In summary, ciliated cells predominate in the fimbria and ampulla of the pig oviducts at the follicular phase of the oestrous cycle, and the numbers and height of ciliated cells is dramatically reduced in the luteal phase. The 'pinching off' of clusters of cilia from the ciliated cells of the fimbriae and ampulla of the CM pig oviduct

appears to be the mechanism for deciliation. Moreover, marked regional variations in ciliation were associated with the cyclic changes. These cytomorphometric and ultrastructural changes were more dramatic in the CM pig than those in the LW pig. Although the reason for these differences between the CM and LW pigs is unclear, it appears that there is a certain relation between the dramatic cyclic changes of oviductal epithelial cells and the prolific breed capacity of CM pig. The biological significance of regional and cyclic variations in ciliation of the CM pig oviduct needs further investigation to improve our understanding of the physiological function of oviductal epithelial cells in the reproductive process.

Acknowledgements

The authors thank Dr S. Sugawara for his generous gift of animals, M. Onodera for his help in obtaining oviductal specimens, and Drs T. Onitake and A. Watanabe for their help with our electron microscopic studies. This work was supported by Grant-in-Aid for Scientific Research (17380164, 18038003) from the Ministry of Education, Culture, Sports, Science and Technology of Japan (to H.A.) and Special Coordination Funds for Promoting Science and Technology.

References

Abe H, 1996: The mammalian oviductal epithelium: Regional variations in cytological and functional aspects of the oviductal secretory cells: Histol Histopathol **11,** 743–768.

Abe H, Hoshi H, 2007: Regional and cyclic variations in the ultrastructural features of secretory cells in the oviductal epithelium of the Chinese Meishan pig: Reprod Domest Anim **42,** 292–298.

Abe H, Oikawa T, 1989: Differentiation of the golden hamster oviduct epithelial cells during postnatal development: an electron microscopic study: J Exp Zool **252,** 43–52.

Abe H, Oikawa T, 1992: Examination by scanning electron microscopy of oviductal epithelium of the prolific Chinese Meishan pig at follicular and luteal phases: Anat Rec **233,** 99–408.

Abe H, Oikawa T, 1993a: Effects of estradiol and progesterone on the cytodifferentiation of epithelial cells in the newborn golden hamster: Anat Rec **235,** 390–398.

Abe H, Oikawa T, 1993b: Observations by scanning electron microscopy of oviductal epithelial cells from cows at follicular and luteal phases: Anat Rec **235,** 399–410.

Abe H, Onodera M, Sugawara S, 1993: Scanning electron microscopy of goat oviductal epithelial cells at the follicular and luteal phases of the oestrous cycle: J Anat **183,** 415–421.

Abe H, Sendai Y, Satoh T, Hoshi H, 1995: Bovine oviduct-specific glycoprotein is a potent factor for the maintenance of the viability and motility of bovine spermatozoa *in vitro*: Mol Reprod Dev **42,** 226–232.

Abughrien BA, Dore MA, 2000: Ciliogenesis in the uterine tube of control and superovulated heifers: Cells Tissues Organs **166,** 338–348.

Akins EL, Morrissette MC, 1968: Gross ovarian changes during estrous cycle of swine: Am J Vet Res **29,** 1953–1957.

Anderson RGW, Brenner RM, 1971: The formation of basal bodies (centrioles) in the rhesus monkey oviduct: J Cell Biol **50,** 10–34.

Bajpai VK, Shipstone AC, Gupta DN, Karkun JN, 1977: Differential response of the ampullary and isthmic cells to ovariectomy and estrogen treatment: An ultrastructural study: Endokrinologie **69,** 11–20.

Bazer FW, Thatcher WW, Martinat-Botte F, Terqui M, 1988a: Conceptus development in Large White and prolific Chinese Meishan pigs: J Reprod Fertil **84,** 37–42.

Bazer FW, Thatcher WW, Martinat-Botte F, Terqui M, 1988b: Sexual maturation and morphological development of the reproductive tract in Large White and prolific Chinese Meishan pigs: J Reprod Fertil **83,** 723–728.

Brenner RM, 1969a: The biology of oviductal cilia. In: Hafez ESE, Blandau RJ, Hafez ESE, Blandau RJ (eds), The Mammalian Oviduct. The University of Chicago Press, Chicago and London, pp. 203–229.

Brenner RM, 1969b: Renewal of oviduct cilia during the menstrual cycle of the rhesus monkey: Fertil Steril **20,** 599–611.

Brenner RM, Resko JA, West NB, 1974: Cyclic changes in oviductal morphology and residual cytoplasmic estradiol binding capacity induced by sequential estradiol-progesterone treatment of spayed rhesus monkeys: Endocrinology **95,** 1094–1104.

Brenner RM, Carlisle KS, Hess DL, Sandow BA, West NB, 1983: Morphology of the oviducts and endometria of cynomolgus macaques during the menstrual cycle: Biol Reprod **29,** 1289–1302.

Cheng P-L, 1984: A highly prolific pig breed of China – The Taihu pig. Part III and IV: Pig News Inf **5,** 13–18.

Dirksen ER, 1971: Centriole morphogenesis in developing ciliated epithelium of the mouse oviduct: J Cell Biol **51,** 286–302.

Dirksen ER, Crocker TT, 1965: Centriole replication in differentiating ciliated cells of mammalian respiratory epithelium. An electron microscopic study: J Microsc **5,** 629–644.

Fredricsson B, Holm S, 1974: Dissociated response of the epithelium of the rabbit oviduct to estrogen: Biol Reprod **11,** 40–49.

Gandolfi F, 1995: Functions of proteins secreted by oviduct epithelial cells: Microsc Res Tech **32,** 1–12.

Gupta DN, Karkun JN, Kar AB, 1969: Studies on physiology and biochemistry of the Fallopian tube: response of the different parts of the rabbit Fallopian tube to estrogen and progesterone: Acta Biol Med Ger **22,** 551–559.

Hunter RHF, 1994: Modulation of gamete and embryonic microenvironments by oviduct glycoproteins: Mol Reprod Dev **39,** 176–181.

Hunter RHF, Flechon B, Flechon JE, 1991: Distribution, morphology and epithelial interactions of bovine spermatozoa in the oviduct before and after ovulation: A scanning electron miscroscope study: Tissue Cell **23,** 641–656.

Komatsu M, Fujita H, 1978a: Electron-microscopic studies on the development and aging of the oviduct epithelium of mice: Anat Embryol **152,** 243–259.

Komatsu M, Fujita H, 1978b: Some observations on ciliogenesis in the oviduct epithelium of the mouse: Arch Histol Jpn **41,** 229–237.

McCarron LK, Anderson E, 1973: A cytological study of the postnatal development of the rabbit oviduct epithelium: Biol Reprod **8,** 11–28.

Nayak RK, Alberts EN, Kassira WN, 1976a: Fine structural changes of the porcine uterine tube epithelium during early and late pregnancy: Am J Vet Res **37,** 1421–1433.

Nayak RK, Albert EN, Kassira WN, 1976b: Ultrastructural studies of prepubertal porcine uterine tube epithelium: Am J Vet Res **37,** 1001–1010.

Nayak RK, Zimmerman DR, Albert EN, 1976c: Electron microscopic studies of estrogen-induced ciliogenesis and secretion in uterine tube of the gilt: Am J Vet Res **37,** 189–197.

Nayak RK, Kassira WN, Albert EN, 1977: Light and electron microscopic studies of the porcine fetal uterine tube (oviduct): Am J Vet Res **37,** 1421–1433.

Odor DL, Blandau RJ, 1973: Egg transport over the fimbrial surface of the rabbit oviduct under experimental conditions: Fertil Steril **24,** 292–300.

Odor DL, Blandau RJ, 1985: Observations on the solitary cilium of rabbit oviductal epithelium: Its motility and ultrastructure: Am J Anat **174,** 37–453.

Odor DL, Gaddum-Rosse P, Rumery RE, Blandau RJ, 1980: Cyclic variations in the oviductal ciliated cells during the menstrual cycle and after estrogen treatment in the pig-tailed monkey, *Macaca nemestrina*: Anat Rec **198,** 35–57.

Pollard JW, Plante C, King WA, Hansen PJ, Betteridge KJ, Suarez SS, 1991: Fertilizing capacity of bovine sperm may be maintained by binding to oviductal epithelial cells: Biol Reprod **44,** 102–107.

Rumery RE, Gaddum-Rosse P, Blandau RJ, Odor DL, 1978: Cyclic changes in ciliation of the oviductal epithelium in the pig-tailed macaque (*Macaca nemestrina*): Am J Anat **153,** 345–366.

Smith TT, Koyanagi F, Yanagimachi R, 1987: Distribution and number of spermatozoa in the oviduct of the golden hamster after natural mating and artificial insemination: Biol Reprod **37,** 225–234.

Sorokin SP, 1968: Reconstructions of centriole formations and ciliogenesis in mammalian lungs: J Cell Sci **3,** 207–230.

Stalheim OHV, Gallagher JE, Deyoe BL, 1975: Scanning electron microscopy of the bovine, equine, porcine, and caprine uterine tube (oviduct): Am J Vet Res **36,** 1069–1075.

Steinman RM, 1968: An electron microscopic study of ciliogenesis in developing epidermis and trachea in the embryo of *Xenopus laevis*: Am J Anat **122,** 19–56.

Suarez S, Redfern K, Raynor P, Martin F, Phillips DM, 1991: Attachment of boar sperm to mucosal explants of oviduct *in vitro*: Possible role in formation of a sperm reservoir: Biol Reprod **44,** 998–1004.

Verhage HG, Brenner RM, 1975: Estradiol-induced differentiation of the oviductal epithelium in ovariectomized cats: Biol Reprod **13,** 104–111.

Verhage HG, Bareither ML, Jaffe RC, Akbar M, 1979: Cyclic changes in ciliation, secretion and cell height of the oviductal epithelium in women: Am J Anat **156,** 505–522.

Wu ASH, Carlson SD, First NL, 1976: Scanning electron microscopic study of the porcine oviduct and uterus: J Anim Sci **42,** 804–809.

Yaniz JL, Lopez-Gatius F, Hunter RHF, 2006: Scanning electron microscopic study of the functional anatomy of the porcine oviductal mucosa: Anat Histol Embryol **35,** 28–34.

Submitted: 09.10.2006

Author's address (for correspondence): Hiroyuki Abe, Tohoku University Biomedical Engineering Research Organization, 6-6-07 Aoba, Aramaki, Aoba-ku, Sendai, Miyagi 980–8579, Japan. E-mail: abe@tubero.tohoku.ac.jp

臨床経験

電気化学的呼吸計測によるヒト胚のクオリティー評価

那須　恵[*1]　熊迫陽子[*1]　後藤（平井）香里[*1]　宇津宮隆史[*1]
荒木康久[*2]　横尾正樹[*3]　阿部宏之[*3]

本研究では，電気化学的計測技術を基盤とする走査型電気化学顕微鏡（SECM）を用い非侵襲的に単一のヒト胚の呼吸量を測定し，胚の呼吸能と形態的クオリティーとの関係を調べた。その結果，Day 3 胚において割球数を基準とする形態的クオリティーと胚の呼吸能の間には明確な相関は認められなかったが，良好な呼吸能を有する胚は測定後の追加培養により高い確率で胚盤胞に発生することが明らかとなった。SECM を用いた呼吸計測法は，細胞の代謝活性能を指標とする新しいヒト胚クオリティー評価法として期待される。

はじめに

現在，体外受精・胚移植の分野において一般的に，卵巣から多数の卵子を回収し，胚移植の際には，複数の胚のなかから移植する胚を選択している。妊娠率の向上，多胎率・流産率を減少させるためには，より着床しうる能力を持った高品質胚を選択することが不可欠である。現在，胚のクオリティー評価は簡単で非侵襲的な方法である形態的評価法が最も普及している。しかし，形態的評価法は観察者の主観により判定結果に差が生じる可能性があるため，より客観的で精度の高い胚クオリティー評価法の開発が望まれている。

筆者らは形態観察に比べてより客観的な方法として，細胞呼吸能測定による胚クオリティー評価方法を提案している。これは，高感度で生体反応を検出できる電気化学的計測技術の基盤である走査型電気化学顕微鏡（SECM）を用いて非侵襲的に胚の呼吸量を測定し，呼吸能を指標に胚のクオリティーを評価する新しい方法である。これまでにウシ胚を用いた研究により，呼吸活性を基準とする胚クオリティー評価法の開発に成功している[1)2)]。さらに，SECM を用いて単一のヒト胚の呼吸量測定に初めて成功している[3)]。そこで本研究では，SECM を用いて Day 2～3 胚（体外受精：Day 0）の呼吸量を測定し，形態的評価との関係を調べた。さらに，呼吸測定胚の追加培養試験を行い，胚の呼吸能と発生能との関係を検討した。

[*1]Megumi NASU, Yoko KUMASAKO, Kaori GOTO, Takafumi UTSUNOMIYA
セント・ルカ産婦人科
[*2]Yasuhisa ARAKI
高度生殖医療技術研究所
[*3]Masaki YOKOO, Hiroyuki ABE,
東北大学先進医工学研究機構生命機能科学分野
〒870-0947　大分県大分市津守富岡5組（セント・ルカ産婦人科）

I. 方　法

1. 材　料

すべて患者の同意が得られた余剰胚を呼吸量測定に供した。凍結保存余剰胚を融解した後，Sydney IVF Cleavage Medium（Cook 社）を用いて 5% O_2，5% CO_2，90% N_2の気相下に 37℃で培養を行った。受精日を Day 0 とし，Day 2

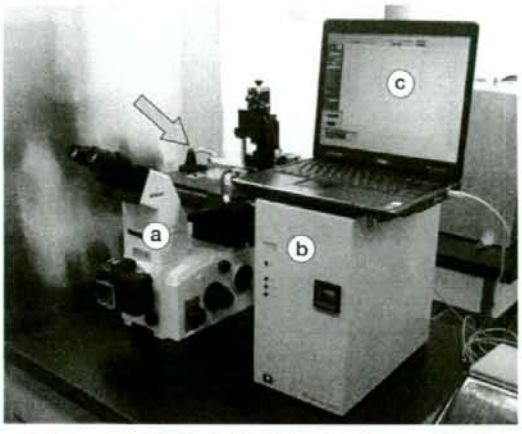

図1　走査型電気化学顕微鏡を改良した「受精卵呼吸測定装置」
ⓐ 倒立型顕微鏡（矢印は測定部を示す）。ⓑ ポテンショスタット。ⓒ ノート型パソコン。

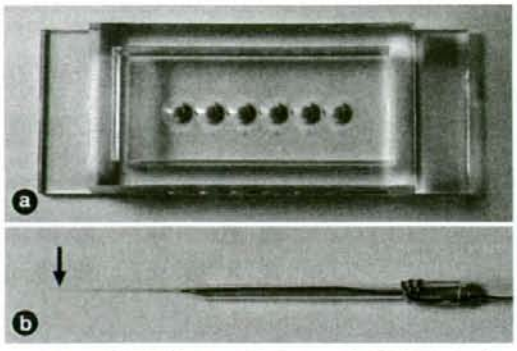

図2　呼吸測定用に開発した多検体測定プレート（ⓐ）とマイクロ電極（ⓑ）
ⓐ 多検体プレート底面には円錐形のマイクロウェルが施されている。ディスク型白金マイクロ電極。先端部（矢印）が直径 2〜4 μm にエッチング加工された白金線がガラスキャピラリー先端部に封止されている。

もしくは Day 3 にて 3〜10 細胞期胚に発生した胚を Veeck の分類法[4]を基に，割球数，細胞の均一性，フラグメンテーションの程度を基準に新たに 1〜4 の 4 段階のグレードに評価した。胚を形態観察により評価した後，SECM をベースに開発した「受精卵呼吸測定装置」を用いて個々の胚の呼吸量を測定した。呼吸測定後，胚発生能を調べるために個々の胚を Day 3 までは Sydney IVF Cleavage Medium（Cook 社）を用いて培養し，Day 4 以降は Sydney IVF Blastocyst medium（Cook 社）に培地交換を行い，Day 5〜7 まで培養し胚盤胞発生率および呼吸量を調べた。

2．呼吸量測定

図 1 に，「受精卵呼吸測定装置」を示す。装置は，XYZ ステージを備えた倒立型顕微鏡，マイクロ電極の電位を一定に保持するポテンショスタット，呼吸解析ソフトを内蔵したノートパソコンにより構成されている。呼吸量の測定には，先端径を 2〜4 μm にエッチング加工した白金をガラスキャピラリーで封止したディスク型マイクロ電極と底部に円錐形のマイクロウェル 6 個を施した専用の測定プレート（図 2）を用いた。測定プレートに 10% synthetic serum substitude（SSS；IS Japan）を添加した modified-human follicle fluid（m-HFF：扶桑薬品工業株式会社）を 5 m*l* 入れ，液温が 37℃になるように保温プレートの温度を調節した。マイクロウェルのなかにミネラルオイルが混入しないように胚を 10% SSS 添加 m-HFF で洗浄した後，マイクロウェルの底部中心に胚を静置した。参照電極を測定プレートの端に設置した後，マイクロ電極を透明帯の間近に移動させた。ポテンショスタットの電位を酸素が還元可能な −0.6 V vs. Ag/AgCl（参照電極）に保持した後，移動速度 30 μm/sec，走査距離 160 μm の条件で透明帯に対して鉛直方向（Z 軸方向）に掃引した。

3．胚の呼吸量

Day 2〜3 における 3〜10 細胞期胚（n＝70）の呼吸量を測定した。各分割期の酸素消費（呼吸）量を表 1 に示す。呼吸量（$F\times10^{14}$/mol s^{-1}）の平均値は，0.33〜0.53 であり各分割期間に顕著な差はなかった。一方，同一分割期において，それぞれの胚の呼吸能に顕著な違いが認められた。例えば，Veeck の分類によって 3 分割グレード 3 と形態的に同じクオリティーと評価された胚の呼吸量を比較した結果，呼吸測定値はそれぞれ 0.94，0.68，0.61，0.19，0.18 であり胚によって顕著な違いがあった。他の分割期におい

表1　異なる分割期におけるヒト胚の酸素消費量（呼吸量）

分割期	測定胚数	酸素消費量（$\times 10^{14}$/mol s^{-1}）
3細胞	5	0.52±0.33
4細胞	3	0.33±0.06
5細胞	6	0.50±0.21
6細胞	13	0.38±0.15
7細胞	15	0.37±0.21
8細胞	20	0.37±0.21
9細胞	4	0.35±0.11
10細胞	4	0.53±0.37

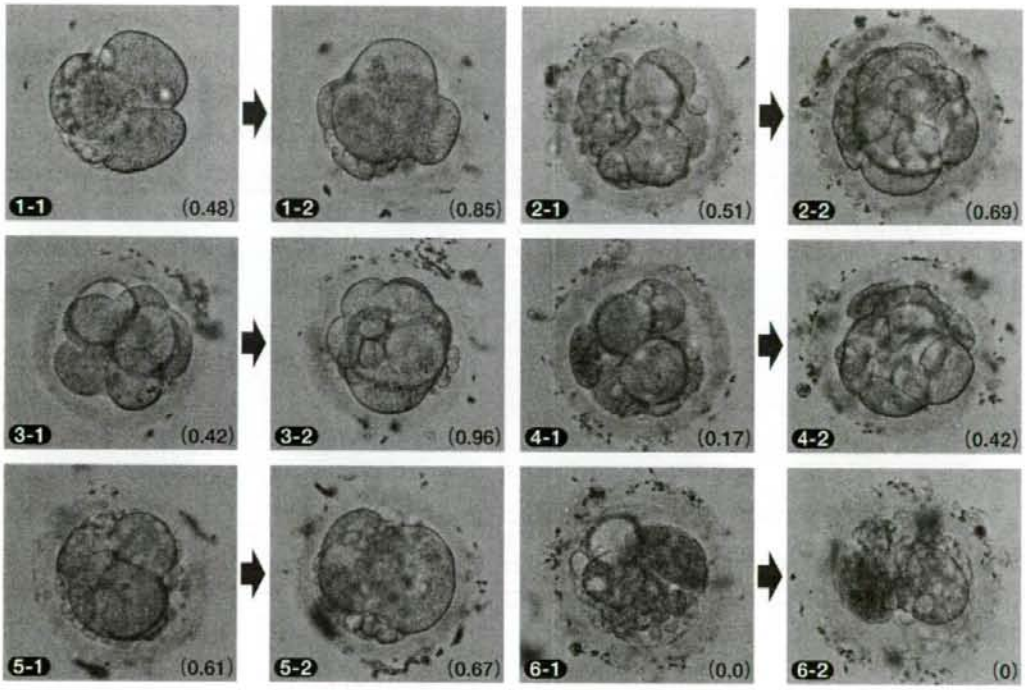

図3　ヒト体外受精胚の形態と呼吸量

受精後3日目のヒト胚（Day 3胚：1-1，2-1，3-1，4-1，5-1，6-1）と呼吸測定後に1日間個別培養したヒト胚（Day 4胚：1-2，2-2，3-2，4-2，5-2，6-2）のそれぞれの光学顕微鏡像と呼吸量（括弧内の数字：$F\times 10^{14}$/mol s^{-1}）を示す。

ても同様の傾向が観察された。このように本研究では，Veeckの分類法による形態的評価と胚の呼吸能には明確な相関は認められなかった。

胚発生と呼吸能の関係を調べるために呼吸測定後の胚（Day 3）を個別に培養し，胚の呼吸量変化を調べた。その結果，培養前に比較的高い呼吸能を有する胚の多くは，培養1日後に発生の進行が観察され呼吸量の増加も認められた（図3）。一方，呼吸能の高い胚の一部や呼吸活性がほとんど検出できない胚では，発生の進行や呼吸量の増加は起こらなかった。次に，Day 3胚を呼吸測定後2日間個別に培養し，呼吸能と胚盤胞発生率の関係を調べた。その結果，Day 3において呼吸量が0.26～0.56$\times 10^{14}$/mol

表2　ヒト胚の呼吸能と胚盤胞発生率の関係

酸素消費量（$F\times10^{14}$/mol s^{-1}）	測定胚数	胚盤胞に発生した胚数(%)
$F>0.56$	14	5（35.7）
$0.26\leqq F\leqq0.56$	65	41（63.1）
$F<0.26$	26	11（42.3）

s^{-1}であった胚は60%以上が胚盤胞に発生した（表2）。一方，呼吸量が0.26×10^{14}/mol s^{-1}以下および0.56×10^{14}/mol s^{-1}以上であった胚の胚盤胞発生率は，それぞれ35.7%，42.3%であった。

II. 考　察

胚移植にあたり，最も良好な胚を選別し，1個移植することは妊娠率の向上，流産率の低下のために不可欠である。これまで，分割期胚の段階でクオリティー良好胚を選別するための形態的判断基準として多くの施設でVeeckの分類[4]が使用されている。さらに，よりクオリティー良好な胚を選択するために様々な判定基準について研究が進められてきた。Zollnerら[5]は前核の接着や前核数の評価に基づく，スコアリングシステムを開発・提案している。Scottら[6]，Tesarikら[7]や公文ら[8]は，前核や核小体の形態による判定を提案している。また，Haydarら[9]は，2細胞期のそれぞれの細胞の核の局在の判定と早期分割による胚発生能の評価法を提案している。しかし，いずれも形態的特徴の観察による評価法であるため，判定結果が観察者の主観によって影響を受ける可能性は否定できない。

1998年頃からは，胚盤胞期用の培養液の作成に成功したことにより胚の成長段階と子宮内の環境を同期化できること，培養期間が長くなることにより移植胚の選別が容易になり，1個か2個の胚を移植することで多胎を防ぐことができるという理由から，胚盤胞期移植が広まった。しかし，一卵性双胎が増加することや，培養期間が長くなるため，胚盤胞まで発育できず発育停止による理由から，胚移植キャンセルになる可能性が高くなるという欠点も持ち合わせている。そのため，大多数の施設ではDAY2もしくはDAY3の分割期胚を移植しているのが現状である。

分割期胚移植と胚盤胞移植の比較検討としては，Gardnerら[10]やScholtesら[11]が，胚盤胞移植を行うことにより着床率は分割期胚移植に比べて有意に上昇したと報告をしている。しかし，Coskunら[12]，Karakiら[13]やUtsunomiyaら[14]により，胚盤胞まで発育が進まず移植キャンセルとなった症例を含めた上での妊娠率は分割期胚移植と有意差はないという報告もなされている。

分割期胚移植の検討としては，受精確認からDAY2移植もしくはDAY3移植の妊娠率の比較を行った結果，Carilloら[15]の妊娠率に差があるという報告の一方，Lavergeら[16]は妊娠率に差はないという報告をした。また，着床率を上げる試みとしては，Cohenら[17]は分割胚を固定し，マイクロピペットにより透明帯を一部切開するassisted hatchingを提案し，長木ら[18]により当院における臨床応用の可能性を検討している。また，Munneら[19][20]は分割胚の状態で割球をFISH法にて染色体を調べた結果，胚の染色体異常はモザイクである頻度が高く，また割球の形が不均等でフラグメンテーションを有している場合，diploidのモザイク，異数性，多数性の頻度が増加すると報告している。また，大津ら[21]は分割胚の割球大小不同と染色体異常の関係についてFISHを用いて検討を行った結果，バイオプシーを行う細胞サイズによって異なる判定が得られる可能性があるということを報告している。染色体がモザイクである割球は発育停止する可能性があり，割球の染色体異常が胚

全体の発生へ及ぼす影響，およびモザイク胚が異常であるかはまだわからないのが現状である。

Abeらは，胚のクオリティーに関連する微細構造の解析を行い，ミトコンドリアが胚のクオリティーに密接に関係していることを発見している[22]。ミトコンドリアは酸化的リン酸化反応（呼吸）により細胞活動に必要なエネルギー（ATP）を産生することから，ミトコンドリアが発達している胚は呼吸活性が高く，一方の不良胚ではミトコンドリアの呼吸代謝能が低いと考えられる。この研究成果を基にAbeらは，高感度・非侵襲的に細胞の呼吸を検出できる電気化学計測技術に着目し，この計測技術の中心であるSECMをベースとする受精卵呼吸測定装置を開発している[1)23)24)]。これまでに，ウシ，ブタ，マウスの単一胚の無侵襲的呼吸能解析に成功しており，呼吸能を指標とする胚クオリティー評価法の有効性を示している[2)]。最近，電気化学的呼吸計測技術のヒト胚への応用を目的に，単一ヒト余剰胚の呼吸量測定を行っている。体外受精後のすべての発生ステージにおいて単一胚の呼吸量測定に成功するとともに，ミトコンドリアの発達と呼吸量の増加が一致することを明らかにしている[3)]。

本研究ではヒト胚の形態と呼吸能との関連性を調べた結果，胚の呼吸能とVeeckの分類法による形態的評価は完全に一致しなかった。しかしながら電気化学計測法は，形態観察では評価できない胚の呼吸能を正確にモニターすることができることから，細胞代謝活性能（ミトコンドリア機能）を指標とする新しい胚クオリティー評価法の基盤技術になると期待される。

おわりに

本研究では，電気化学的呼吸測定技術を応用した新しいヒト胚クオリティー評価の可能性が示された。胚の呼吸測定と形態的評価を併用することで，より厳密に胚のクオリティーを評価できる可能性がある。今後，胚のクオリティーと呼吸能との関係を詳しく調べるとともに，呼吸測定の有効性と安全性を検討し，呼吸測定技術および装置の臨床応用を目指したい。

文　献

1) Abe H, Shiku H, Aoyagi S, et al : *In vitro* culture and evaluation of embryos for production of high quality bovine embryos, J Mamm Ova Res, **21** : 22-30, 2004.
2) Abe H, Shiku H, Aoyagi S, et al : Evaluating the quality of individual embryos with a non-invasive and highly sensitive measurement of oxygen consumption by scanning electrochemical microscopy, J Reprod Dev, **52** (Suppl): S55-S64, 2006.
3) 阿部宏之，横尾正樹，荒木康久，他：電気化学的イメージング法を応用した単一ヒト胚の呼吸能解析，産婦の実際，**56**：2053-2057, 2007.
4) Veeck LL : Atlas of the Human Oocyte and Early Conceptus, Vol. 2, Willams & Wilkins, Baltimore, 1991.
5) Zollner U, Zollner KP, Hartl G, et al : The use of a detailed zygote score after IVF/ICSI to obtain good quality blastocysts : the German experience. Hum. Reprod, **17** : 1327-1333, 2002.
6) Scott L, Alvero R, Leondires M, et al : The morphology of human pronuclear embryos is positively related to blastocyst development and implantation. Hum Rsprod, **15** : 2394-2403, 2000.
7) Tesarik J, and Greco E : The probability of abnormal preimplantation development can be predicted by a single static observation on pronuclear stage morphology. Hum Replod, **14** : 1318-1323, 1999.
8) 公文麻美，大津英子，長木美幸，他：前核期胚における形態的評価の検討，第58回日本不妊学会九州支部会抄録集，2001.
9) Haydar NC, Levent K, Ulun U, et al : Early cleavage morphology affects the quality and implantation potential of day 3 embryos. Fertil Steril, **85** : 358-365, 2006.
10) Gardner DK, Schoolcraft WB, Wargley L, et al : A prospective randomized trial of blastocyst culture and transfer in *in-vitro* fertilization. Fertil Steril, **13** : 3434-3440, 1998.
11) Scholtes MC, Zeilmaker GH : Blastocyst transfer in day-5 embryo transfer depends primarily on the number of oocytes retrieved and not on age. Fertil Steril, **69** : 78-83, 1998.
12) Coskun S, Hollanders J, Al-Hassan S, et al : Day-5

versus day-3 embryo transfer ; a controlled randomized trial. Hum Reprod, **15** : 1947-1952, 2000.
13) Karaki RZ, Samarraie SS, Younis NA, et al : Blastocyst culture and transfer ; a step toward improved *in vitro* fertilization outcome. Fertil Steril, **77** : 114-118, 2002.
14) Utsunomiya T, Ito H, Nagaki M, et al : A Prospective, Randomized Study : Day-3 versus Hatching Blastocyst Stage. Hum Reprod, **19** : 1598-1603, 2004
15) Carillo AJ, Lane B, Pridham DD, et al : Improved clinical outcomes for *in vitro* fertilization with delay of embryo transfer from 48 to 72 hours after oocyte retrieval ; use of glucose-and phosphate-free media. Fertil Steril, **69** : 329-334, 1998.
16) Laverge H, De Sutter P, Van der Elst J, et al : A prospective, randomized study comparing day 2 and day 3 embryo transfer in human IVF. Hum Reprod, **16** : 476-480, 2001.
17) Cohen J, Elsner C, Kort H, et al : Impairment of the hatching process following IVF in the human and improvement of implantation by assisted hatching using micromanipulation. Hum Reprod, **5** : 7-13, 1990.
18) 長木美幸，佐藤真紀，広津留恵子，他：当院における凍結・融解胚移植の成績，第53回日本不妊学会九州支部会抄録集，1999.
19) Munne S, Alikani M, Tomkin G, et al : Embryo morphology, developmental rates, and maternal age are correlated with chromosome abnormalities. Fertil Steril, **64** : 382-391, 1995.
20) Munne S, Cohen J : Chlomosome abnormalities in human embryos. Hum Reprod Update, **4** : 842-855, 1998.
21) 大津英子，佐藤晶子，長木美幸，他：ヒト胚における割球大小不同と染色体異常の関係，日受精着床会誌，**24** : 34-37, 2007.
22) Abe H, Matsuzaki S, Hoshi H : Ultrastructural differences in bovine morulae classified as high and low qualiies by morphological evaluation. Theriogenology, **57** : 1273-1283, 2002.
23) Shiku H, Shiraishi T, Ohya H, et al : Oxygen consumption of single bovine embryos probed with scanning electrochemical microscopy, Anal Chem, **73** : 3751-3758, 2001
24) Shiku H, Shiraishi T, Aoyagi S, et al : Respiration activity of single bovine embryos entrapped in a cone-shaped microwell monitored by scanning electrochemical microscopy, Anal Chim Acta, **522** : 51-58, 2004.

お詫びと訂正＊＊＊＊＊＊＊＊＊＊＊＊＊＊＊＊＊＊＊＊＊＊＊＊＊＊＊＊＊＊

『産婦人科の実際』57巻1号，原著欄「子宮内膜症と子宮筋腫に対する偽閉経療法としての酢酸リニューブロレリン，酢酸ゴセレリン，酢酸プセレリンのランダム化試験(中間報告)」中に誤りがございました。下記のように訂正させて頂きますとともに，お詫び申し上げます。

109頁右段下から7行目

誤	正
2003年4月～2005年9月	2003年4月～2006年9月

＊＊＊＊＊＊＊＊＊＊＊＊＊＊＊＊＊＊＊＊＊＊＊＊＊＊＊＊＊＊＊＊＊＊＊＊

—Mini Review—

Evaluating the Quality of Human Embryos with a Measurement of Oxygen Consumption by Scanning Electrochemical Microscopy

Takafumi Utsunomiya[1]*, Kaori Goto[1], Megumi Nasu[1], Yoko Kumasako[1], Yasuhisa Araki[2], Masaki Yokoo[3], Takahiro Itoh-Sasaki[4] and Hiroyuki Abe[4]

[1]St-Luke Clinic, 5 Tsumori Tomioka, Oita City, Oita 870-0947, Japan
[2]The Institute for ARMT, Gunma 371-0105, Japan
[3]Innovation of New Biomedical Engineering Center, Tohoku University, Sendai 980-8574, Japan
[4]Graduate Program of Human Sensing and Functional Sensor Engineering, Graduate School of Science and Engineering, Yamagata University, Yonezawa 992-8510, Japan

Abstract: Morphological evaluation has been widely used to evaluate embryo quality because it is non-invasive and useful in predicting pregnancy rate. However, morphological evaluations are subjective and categorization standards often vary between investigators. The respiration rate of embryos is a useful parameter for evaluating embryo quality. The scanning electrochemical microscopy (SECM) measuring system provides a non-invasive, simple, accurate, and consistent measurement of the respiration activity of human embryos. After morphological evaluation by Veeck's method, oxygen consumption by individual human embryos was quantified by SECM. Fundamentally, the maturation of mitochondria correlated with an increase in oxygen consumption during the development of embryos. The development of mitochondria may be an important factor in embryo quality, because mitochondria provide ATP for embryonic development by metabolism of nutrients in the cytoplasm. The respiration rates on the day 3 after in vitro fertilization (IVF) were measured and significant differences in oxygen consumption were registered even among embryos with the same morphological classification. There were no significant differences between the mean rates of oxygen consumption at each cleavage stage, however, there was considerable variation in respiration rate within embryos of the same morphological grade. The safety of SECM is assured as the embryos which were examined by SECM for oxygen consumption showed the same development levels as the control group. These results support the hypothesis that measuring embryonic respiration provides additional and valuable information about embryo quality.

Key words: Embryo quality, Oxygen consumption, Non-invasive evaluation

Received: January 19, 2008
Accepted: February 22, 2008
*To whom correspondence should be addressed.
e-mail: st-luke@oct-net.ne.jp

Introduction

Morphological evaluation has been widely used to evaluate embryo quality because it is non-invasive and useful in predicting pregnancy rates. However, morphological evaluations are subjective and categorization standards often vary among investigators. Therefore, more objective selection criteria are needed. Respiration is a useful parameter for evaluating embryo quality as it provides important information about metabolic activity. The scanning electrochemical microscopy (SECM) measuring system, which was introduced by Abe *et al.* [1], provides a non-invasive, simple, accurate, and consistent measurement of the respiration activity of single human embryos.

Scanning electrochemical microscopy is a technique in which the tip of a microelectrode is used to monitor the local distribution of electro-active species near the sample surface. The SECM measuring system has

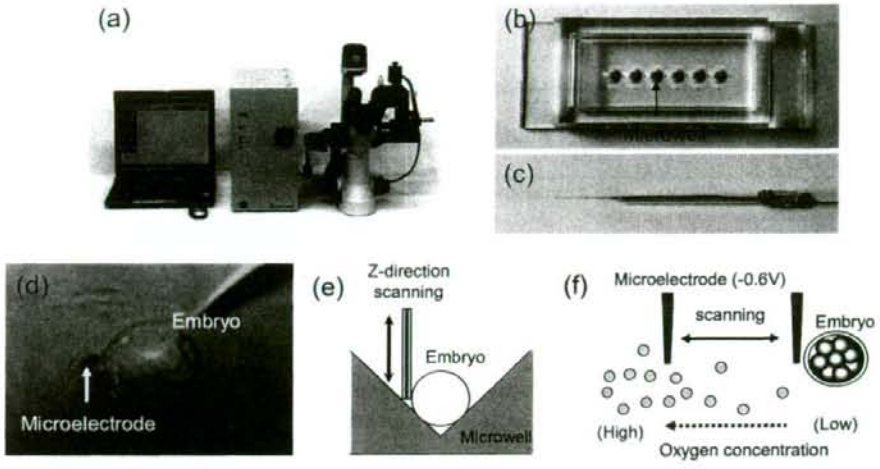

Fig. 1. The SECM system (a), a plate with microwells (b), and a microelectrode (c) for measurement of respiration activity of embryos. SECM includes a measurement instrument on the inverted optical microscope stage, a potentiostat, and notebook computer. The plate has six cone-shaped microwells (arrow). Individual embryos are transferred into a microwell filled with HFF99 medium. The sample sinks to the bottom of the well remaining at the lowest point (d, e). The oxygen concentration profiles are calculated with custom software based on spherical diffusion theory (f). Measurements of each embryo are performed very rapidly.

been used to non-invasively measure respiration activity of single bovine and murine embryos, among other species [2]. We employed SECM to accurately determine the oxygen consumption of single, identical human embryos at different developmental stages. In this article, we introduce the SECM method for assessing the quality of individual human embryos.

Measuring Respiration Activity of Single Human Embryo

Following *in vitro* fertilization (IVF)-embryo transfer procedure, surplus embryos that patients preferred not to keep preserved were used in our study. Informed consent for use of the embryos in this research was obtained from all the patients. From July 2006 to July 2007, 188 embryos from 73 cycles were examined. The mean age of the embryo donor was 34.5 ± 4.5 years and the number of previous ART cycles was 2.7 ± 2.3.

The embryos were cultured in Cleavage Medium (Sydney IVF, Australia) until day 3, after which they were cultured in Blastocyst Medium (Sydney IVF, Australia). After morphological evaluation by Veeck's method, oxygen consumption of individual human embryos was quantified with a modified SECM measuring system (Fig. 1). A single embryo was transferred into a well filled with HFF99 (Fuso Pharmaceutical Industries, Osaka, Japan) medium, where it fell to the bottom of the cone-shaped microwell and remained at the lowest point. A platinum (Pt)-microdisk electrode was lowered into the solution, and its tip potential was held at –0.6V vs Ag/AgCl with a potentiostat to monitor the local oxygen concentration. The microelectrode scanned along the z-axis from the edge of the sample and the oxygen consumption rate was calculated with custom software based on spherical diffusion theory. Measurements of each embryo were performed very rapidly (within 1 min). A part of each embryo was prepared for observation by transmission electron microscopy. The safety of SECM on the embryos was also examined.

The mean respiration rates ($F \times 10^{14}$/mol·s^{-1}) of 4-cell, 5-cell, 6-cell, 7-cell, 8-cell, 9-cell, and 10-cell embryos were 0.34 ± 0.1 (n=8), 0.45 ± 0.2 (n=15), 0.37 ± 0.1

Table 1. Oxygen consumption rates at each cleavage stage

Cleavage stage	No. of embryos examined	Oxygen consumption ($F \times 10^{14}$/mol·s^{-1})
4-cell	8	0.34 ± 0.1
5-cell	15	0.45 ± 0.2
6-cell	39	0.37 ± 0.1
7-cell	51	0.39 ± 0.2
8-cell	50	0.40 ± 0.2
9-cell	12	0.40 ± 0.1
10-cell	12	0.50 ± 0.2

There were no significant differences in the mean rates of oxygen consumption at each cleavage stage.

(n=39), 0.39 ± 0.2 (n=51), 0.40 ± 0.2 (n=50), 0.41 ± 0.1 (n=12), and 0.50 ± 0.2 (n=12), respectively (Table 1). There were no significant differences between the mean respiration rates at each cleavage stage; however, there was considerable variation in respiration rate within embryos of the same morphological grade.

The relationship between the embryo morphology and oxygen consumption was examined (Fig. 2). Significantly different levels of oxygen consumption were registered even among embryos of the same morphological classification.

After measuring their respiration rates with SECM, embryos were cultured to examine their developmental capacity. Embryos with moderate respiration rates (more than 0.26 × 10^{14} /mol·s^{-1} and under 0.56 × 10^{14}/mol·s^{-1}) had a 65.8% chance of reaching the blastocyst stage. On the other hand, embryos with lower (under 0.25 × 10^{14}/mol·s^{-1}) and higher (more than 0.55 × 10^{14}/mol·s^{-1}) respiration rates had only a 39.0% chance of reaching the blastocyst stage (Fig. 3).

The safety of SECM is assured as the embryos which were examined by SECM for oxygen consumption showed the same levels of development as the control group (Fig. 4).

Future Application of SECM in Assisted Reproductive Technology

Finding embryos of the highest quality is an imperative for obtaining good results in ART. To obtain a good embryo, many reports have proposed new methods and findings. A report on the correlation between first polar body morphology and pregnancy rate suggested that preselection at a very early stage may be helpful in identifying a subgroup of preimplantation embryos with good prognosis to form

Individual human embryos on DAY3 after IVF and oxygen consumption rate.

	I	II	III	IV	V	VI
Morphology of embryos						
Classification by Veeck method	4-cell Grade 1	4-cell Grade 1	6-cell Grade 2	6-cell Grade 2	8-cell Grade 2	8-cell Grade 2
Oxygen consumption ($F \times 10^{14}$/mol·s^{-1})	0.25	0.44	0.57	0.23	0.71	0.35

Fig. 2. Individual human embryos on Day 3 after IVF were classified by the method of Veeck *et al.* There were considerable variations in respiration rates within embryos (I and II, III and IV, V and VI) classified as the same morphological grade.